AFRL-RY-WP-TR-2019-0301

SEMI-CLASSICAL AND QUANTUM TRANSPORT FOR HIGH SPEED AND HIGH POWER ELECTRONIC AND OPTO-ELECTRONIC DEVICES

Matthew Grupen

Electronic Devices Branch
Aerospace Components & Subsystems Division

JANUARY 2020
Final Report

AIR FORCE RESEARCH LABORATORY
SENSORS DIRECTORATE
WRIGHT-PATTERSON AIR FORCE BASE, OH 45433-7320
AIR FORCE MATERIEL COMMAND
UNITED STATES AIR FORCE

REPORT DOCUMENTATION PAGE

Form Approved
OMB No. 0704-0188

1. REPORT DATE *(DD-MM-YY)*	2. REPORT TYPE	3. DATES COVERED *(From - To)*
January 2020	Final	17 October 2019 –17 October 2019

4. TITLE AND SUBTITLE
SEMI-CLASSICAL AND QUANTUM TRANSPORT FOR HIGH SPEED AND HIGH POWER ELECTRONIC AND OPTO-ELECTRONIC DEVICES

5a. CONTRACT NUMBER
17RYCOR495

5b. GRANT NUMBER

5c. PROGRAM ELEMENT NUMBER
N/A

6. AUTHOR(S)
Matthew Grupen

5d. PROJECT NUMBER
N/A

5e. TASK NUMBER
N/A

5f. WORK UNIT NUMBER
N/A

7. PERFORMING ORGANIZATION NAME(S) AND ADDRESS(ES)

Air Force Research Laboratory
Sensors Directorate (AFRL/RYDD)
Wright-Patterson Air Force Base, OH 45433-7320
Air Force Materiel Command
United States Air Force

8. PERFORMING ORGANIZATION REPORT NUMBER

9. SPONSORING/MONITORING AGENCY NAME(S) AND ADDRESS(ES)

Air Force Research Laboratory
Sensors Directorate
Wright-Patterson Air Force Base, OH 45433-7320
Air Force Materiel Command
United States Air Force

Air Force Office of Scientific Research Public Affairs (AFOSR)
875 North Randolph Street, Suite 325, Room 3112
Arlington, VA 22203

10. SPONSORING/MONITORING AGENCY ACRONYM(S)
AFRL/RYDD

11. SPONSORING/MONITORING AGENCY REPORT NUMBER(S)
AFRL-RY-WP-TP-2019-0301

12. DISTRIBUTION/AVAILABILITY STATEMENT
Approved for public release; distribution is unlimited.

13. SUPPLEMENTARY NOTES
PAO case number 88ABW-2019-5008, Clearance Date 17 October 2019. This is a work of the U.S. Government and is not subject to copyright protection in the United States. Report contains color.

14. ABSTRACT

This report describes approaches and recent progress for different components of the lab task. This includes addressing the microscopic, fully quantum-mechanical nature of material systems whose electronic properties may be promising for device applications. Incorporating these properties into device simulations that produce experimentally observed behavior is also described. Methods for assessing devices' suitability for circuit applications are considered as well.

15. SUBJECT TERMS
computer simulation

16. SECURITY CLASSIFICATION OF:			17. LIMITATION OF ABSTRACT:	18. NUMBER OF PAGES	19a. NAME OF RESPONSIBLE PERSON (Monitor)
a. REPORT	b. ABSTRACT	c. THIS PAGE			Matthew Grupen
Unclassified	Unclassified	Unclassified	SAR	15	19b. TELEPHONE NUMBER *(Include Area Code)* N/A

Annual Laboratory Task Report 2019

Title:	**Semi-classical and Quantum Transport for High Speed and High Power Electronic and Opto-electronic Devices**
Laboratory Task Manager:	Dr. Matt Grupen
Phone Number:	937-713-8191
Mailing Address:	AFRL/RYDD, 2241 Avionics Circle, Wright-Patterson AFB, OH 45433
E-Mail Address:	Matthew.Grupen@us.af.mil
AFOSR Program Manager:	Dr. Arje Nachman (AFOSR/RTB) Phone: 703-696-8427

1 Air Force Requirements & Research Objectives

The vast range of Air Force technological requirements includes electronic and opto-electronic components and systems operating at high power levels and high frequencies. For example, generating, detecting, and processing high frequency signals for imaging, radar, spectroscopy, and communications require high speed power amplifiers, ultra-linear mixers, and high power digital to analog converters [1–4]. Other applications such as optical communications, laser detection and ranging (ladar), laser imaging, diagnostics, material processing, and infrared countermeasures require high power continuous wave and pulsed optical sources [5, 6]. These capabilities, along with advances in chemical sensing, biological agent detection, and infrared photochemistry, can also benefit from optical sources offering compactness, reliability, and low production costs [7–14].

To meet performance requirements for the Air Force's electronic and opto-electronic applications, material compositions along with device and circuit architectures are continually evolving, creating an enormous design space to explore. Predictive modeling and simulation based on the first principals of physics can provide cost-effective means for better spanning this parameter space to identify promising designs prior to manufacturing [4]. However, such simulation also presents a formidable multi-scale computational physics problem. This lab task investigates new computational approaches that may assist in these atoms-to-systems design challenges and help maintain Air Force technological superiority.

This report describes approaches and recent progress for different components of the lab task. This includes addressing the microscopic, fully quantum-mechanical nature of material systems whose electronic properties may be promising for device applications. Incorporating these properties into device simulations that produce experimentally observed behavior is also described. Methods for assessing devices' suitability for circuit applications are considered as well.

2 Research Approaches

Multi-scale physics problems addressed by this lab task require different approaches including the fully quantum mechanical treatment of solid-state crystals, semi-classical transport of charges through devices made from these materials, and mathematical abstractions capturing device behavior within integrated circuit and system environments. This section introduces some of the approaches to these different parts of the design problem.

2.1 Microscopic Material Properties

Electronic material properties are computed with various quantum mechanical approaches including ab initio software tools available through the Department of Defense's High Performance Computing Modernization Program (HPCMP). For example, the electronic band structure showing available electron energy states can be computed for better known electronic materials, e.g. Si and GaAs, using the empirical pseudopotential method [15, 16]. Electron coupling to lattice vibrations can be computed from their relatively simple acoustic and optical phonon spectra [17] and from known deformation potentials [18] providing intravalley and intervalley electron-phonon scattering rates.

Lesser understood materials may require ab initio methods such as density functional theory (DFT) [19, 20] available in computational quantum chemistry software packages, e.g. Quantum Espresso (QE) and

the Vienna Ab-initio Simulation Package (VASP), supported by the HPCMP. These codes can provide electronic band structures for complex crystal lattices like monoclinic β-Ga_2O_3. Additional features such as the Wannier electron phonon wavefunction [21] utility allow code suites like QE to compute electron-phonon coupling.

2.2 Device Simulation

Incorporating computed electronic material properties into a high speed electron device simulation required developing new computational approaches and tools currently unavailable in the public domain. The general idea is to treat mobile charges in a semiconductor as a gas of particles confined to a phase space. The particle ensembles are forced to obey the laws of an ideal Fermi gas. The phase space is determined by the fully quantum mechanical methods described above.

The various thermodynamic properties of the Fermi gases are determined by integrating their distribution functions over properties of the phase space they occupy. For example, a Fermi gas's electron density is given by,

$$n_i = \int_{E_i} f_i(E) \left[\int_{\boldsymbol{k}_i} \frac{1}{4\pi^3} \frac{\delta(E_{\boldsymbol{k}} - E)}{|\nabla_{\boldsymbol{k}} E|} d\boldsymbol{k} \right] dE = \int_{E_i} f_i(E) \left[\int_{\boldsymbol{k}_i} \rho_{\boldsymbol{k}}(E) d\boldsymbol{k} \right] dE, \tag{1}$$

where f_i is the Fermi distribution and $\nabla_{\boldsymbol{k}} E$ is the gradient of electron energy in the region of $\boldsymbol{k}$-space containing the gas. The flux of Fermi gas particles through phase space is given by the first moment of the Boltzmann equation in the relaxation approximation

$$\boldsymbol{J}_i = \int_{E_i} \left[\int_{\boldsymbol{k}_i} \boldsymbol{v}\boldsymbol{v}^T \tau_{\boldsymbol{k}} \rho_{\boldsymbol{k}}(E) \right] \left(q\boldsymbol{E} \frac{\partial f_i}{\partial E} - \nabla f_i \right) dE, \tag{2}$$

where $\boldsymbol{v} = \nabla_{\boldsymbol{k}} E/\hbar$ and $\tau_{\boldsymbol{k}}$ is the inverse of momentum randomization rates summed over all scattering mechanisms. The bracketed terms in (1) and (2) are pre-computed from the electronic band structure, saved as energy spectra, and read into the device simulation to compute electron densities and fluxes. In this way, the Fermi kinetics transport (FKT) model developed by this lab task captures electronic band structure effects missing from other energy transport models.

2.3 Circuits and Systems

Although the device simulations developed by this lab task can accurately compute electronic device behavior, determining how large numbers of these devices perform together in a highly integrated circuit requires simpler mathematical descriptions that are more computationally efficient. These are often referred to as compact or behavioral models [22]. They can have a variety of different forms, and they are generally empirical in nature.

One type of compact model is the equivalent circuit [23–26], an assembly of mathematical abstractions such as inductors, capacitors, resistors, and voltage controlled current source whose parameters are adjusted to match a device's measured behavior or the behavior computed by the device simulations described above. A closely related approach, often called the charge control model or a "physics-based" equivalent circuit [27–30], assigns functional dependencies of the model's lumped parameters that are motivated by a physical relationship such as Poisson's equation.

Another compact model treats the device as a featureless black box characterized by a frequency-dependent transfer matrix providing output voltage waves in response to specified input waves. The elements of the transfer matrix are called S-parameters as the black box acts as a scattering center for the incident voltage waves. The polyharmonic distortion model generalizes this approach by mapping complex multitone sinusoidal input signals to output signals [31–34]. The weighting factors relating the input and output are called X-parameters [35–42]. They are nonlinear supersets of S-parameters in that S-parameters represent a linearization of the device around a DC quiescent bias point while X-parameters can be viewed as a linearization about a DC bias plus a large amplitude incident voltage wave.

An additional type of compact model considered by this lab task is the neural network [43–45]. These are mathematical constructs that use the device characteristics, measured experimentally or computed by the device simulator from the previous section, to "learn" how their electrical properties respond to design variations. If the instructional data set is large enough and the behavioral model is complex enough, i.e. sufficient degrees of freedom, this can be effective for computer aided engineering. This lab task explores aspects of all the compact model types described here.

3 Program Accomplishments

During this reporting period, progress was made on all fronts of the LRIR's multi-scale simulation effort. This section summarizes useful results for microscopic material properties, device level simulations, and device characterization for power amplifier circuits.

3.1 β-Ga_2O_3 Band Structure and Defects

The monoclinic β-Ga_2O_3 crystal has attracted attention for chemical gas sensing applications [46, 47] and power electronics [48, 49]. However, because of its large and complex primitive unit cell, accurate computation of electronic properties for this crystal requires DFT with hybrid exchange correlation energy functionals involving expensive Hartree-Fock calculation of nonlocal exchange energy [20, 50]. When investigating higher dimensional defects (dislocation or interface), interaction between defects, or configuration order in alloys, a more computationally efficient approach addressing larger scale β-Ga_2O_3 systems may be necessary. Semiempirical methods with various approximations of electronic integrals can lead to significant reduction in computational demand. Among them, the density functional tight binding (DFTB) method is one popular choice derived from DFT [51]. A new parameter set was constructed and optimized for the bulk electronic properties and lattice structure of β-Ga_2O_3. It was also tested for other properties such as surface energy and point defect formation energy.

The first step of parameterization is the pseudoatomic orbital (PAO) of gallium and oxygen. Assuming a quadratic confinement potential of $V_{\text{conf}}(r) = (r/r_0)^2$, the confinement length r_0 becomes an independent parameter of PAO optimization. For a specified confinement length, a set of PAOs (s and p orbitals of oxygen along with s, p, and d orbitals of gallium) can be computed. Using those PAO, Slater-Koster (SK) functions are calculated as functions of separation distance between PAOs [52]. Figure 1 shows the band structure calculation compared with the work of Peelaers and Van de Waale which reported an accurate

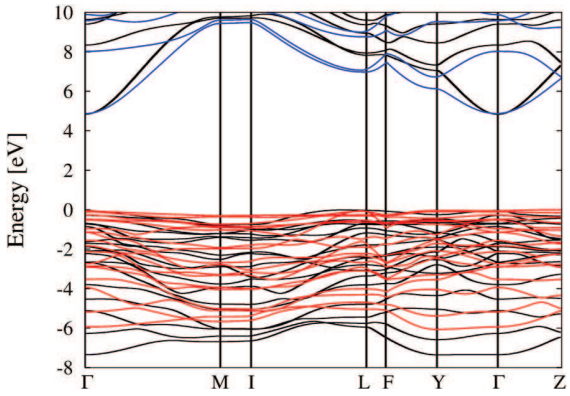

Figure 1: Electronic band structure computed with parameterized DFTB for the conduction (blue) and valence (red) bands. For comparison, the gray lines were computed with DFT by Peelaers and Van de Walle [20].

electronic structure of β-Ga_2O_3 based on DFT with hybrid functional (HSE06) along symmetry lines [20]. The eigenvalues at special points are in reasonable agreement, while the effective carrier mass is overestimated in DFTB.

Figure 2 shows the formation energy of oxygen vacancy defects. All three types of vacancies assume neutral states as stable when the Fermi level is near the conduction band. The donor states of +2 valence become stable in the midgap. The transition level, $\epsilon(+2/0)$, is deeper than 1 eV from the conduction band for all three types of oxygen sites. Such observations are in accordance with well referenced DFT studies [50,53]. However, the formation energies of oxygen vacancies are generally overestimated compared to the reported values of previous DFT studies. Figure 2 also shows the formation energies of gallium vacancy defects, which are in good agreement with the literature [50].

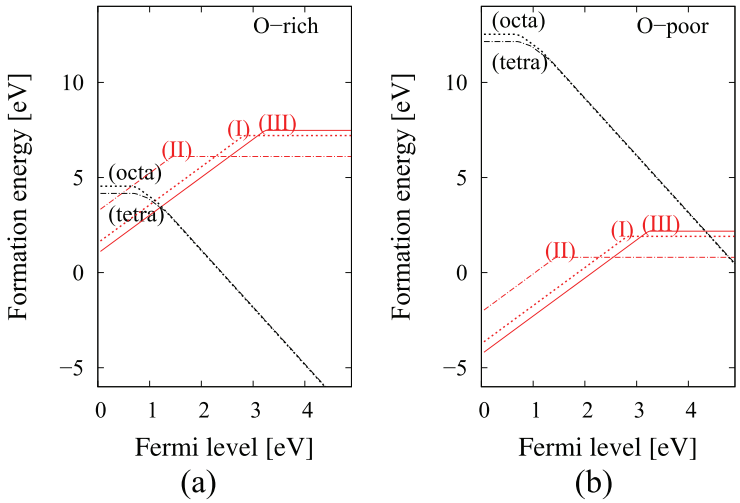

Figure 2: Formation energies of point defects in β-Ga_2O_3 plotted against the Fermi level for (a) oxygen rich and (b) oxygen poor conditions. Red lines are for oxygen defects. Black lines are for gallium vacancies. (tetra) is for vacancy at the Ga(I) site, and (octa) is for vacancy at the Ga(II) site of the monoclinic unit cell.

3.2 GaN HEMT 'Kink' Effect

Efficient, low noise, and linear power amplifiers operating at microwave and mm-wave frequencies are required for a broad range of commercial and defense-related applications such as those cited in Section 1. Wide band gap, high breakdown voltage and heat capacity, good thermal conductivity and electron mobility, as well as a high peak electron velocity [54] make GaN well suited for these applications. Furthermore, the spontaneous and piezoelectric polarizations of the GaN/AlGaN material system can produce a highly conductive two-dimensional electron gas in a high electron mobility transistor (HEMT) structure [55]. For these reasons, the GaN HEMT currently plays a dominant role in RF power amplifier applications [56–60].

Despite its many merits, utilizing the GaN HEMT to its fullest potential requires understanding an operational instability often called the kink effect [61–68]. During a drain voltage sweep, the drain current in the saturation region can appear to be initially suppressed and then increase, over a relatively narrow voltage range, to a higher saturation value. This behavior is concerning, particularly for RF power amplifier design, because the available RF power can be significantly lower than dc characterization might suggest.

To investigate this operational instability, the FKT simulator developed by this lab task was further generalized to include field-enhanced direct quantum mechanical tunneling ionization of deep traps and applied to a device from the literature designed specifically for studying the kink effect [61]. The simulation computed the drain current I_D versus drain voltage V_D for different gate biases V_G shown in Figure 3 (left) along with measured data from Wang and Chen [61]. The kinks in the simulated drain currents are caused by the direct tunneling ionization of sheet traps under the gate on the AlGaN side of the GaN/AlGaN interface that defines the device's channel. A principal reason for the tunneling ionization and its voltage dependence is the highly nonlinear field-dependent tunneling probability plotted along the GaN/AlGaN interface in Figure 3 (right) for different drain voltages. The sudden increase in positively ionized traps has an effect much like an increase in polarization charge at the GaN/AlGaN interface, causing a sudden decrease in threshold voltage and a kink in the drain current.

In addition to field-dependent tunneling probability, hot electrons also play an important role in the defect ionization that causes the kink effect. Figure 4 (left) shows that electron heating in the GaN HEMT biased in saturation is substantial. Electron heating stretches the electron distribution to higher energies, increasing thermal velocity and leaving more low energy states vacant for trap emission, thereby providing the conditions necessary for the kink effect. These consequences of hot electrons are evident in Figure 4 (right), which shows the occupied barrier trap ionization rate normalized by the tunneling probability. Comparing the results with and without electron heating shows the increased thermal velocities and higher average energies of hot electrons increased the ionization rate by orders of magnitude. Along with the highly nonlinear field-dependent tunneling probabilities in Figure 3 (right), these consequences of intense electron heating are essential for the kink effect. Therefore, simulating this GaN HEMT behavior requires a charge

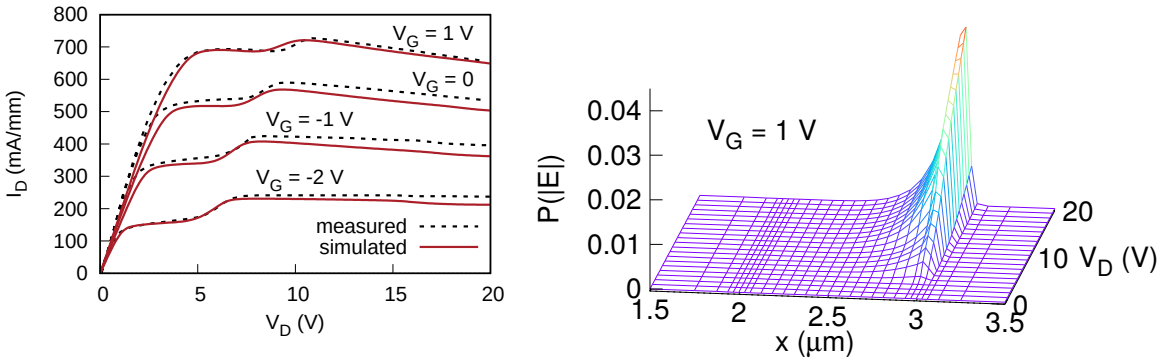

Figure 3: (left) Drain current I_D versus drain voltage V_D for different gate biases V_G. Simulations include field-enhanced ionization of barrier traps under the gate near the GaN/AlGaN interface. The measured data was published by Wang and Chen [61]. (right) The quantum tunneling probability computed along the GaN HEMT channel for gate voltage $V_G = 1$ V and different drain voltages V_D. The position of the gate, where tunneling ionization of barrier defects produces the kink effect, is locate at $2 < x < 3$ μm.

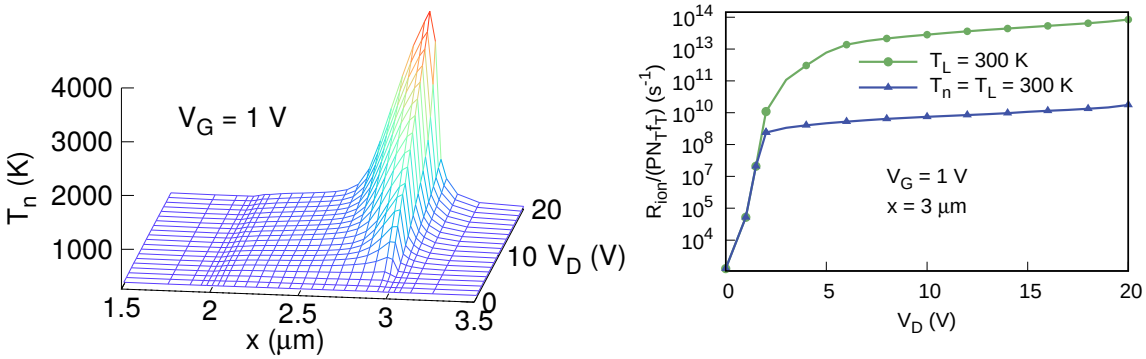

Figure 4: (left) Γ-valley mobile electron temperatures T_n along the channel of the GaN HEMT computed with no lattice heating for gate voltage $V_G = 1$ V and different drain voltages V_D. The gate is located at $2 < x < 3$ μm. (right) The ionization rate normalized by quantum tunneling probability at different drain voltages V_D for an occupied barrier trap on the drain side of the gate computed for gate voltage $V_G = 1$ V. The dot and triangle lines were computed with and without hot electrons, respectively.

transport model that can capture the marked electron heating evident in Figure 4 (left) in a manner that resolves both sub-picosecond hot electron scattering and the widely disparate deep trap ionization time scales indicated in Figure 4 (right). For these reasons, *the FKT simulation produced through AFOSR support appears to be the only computation currently able to capture this operational instability.*

3.3 Device Characterization for Circuit Applications

The extremely crowded electromagnetic environment today demands an increase in the fundamental transistor dynamic range. The inherent power density and linearity are critical large-signal metrics which must be maximized in order to expand the transistors core dynamic range. Not only must new transistor technologies be developed to address today's RF needs, but the operating conditions of these transistors must be optimized to provide peak MMIC performance.

Peak performance often requires maximizing one or more competing metrics such as the output power, power-added efficiency (PAE), and the linearity of the device. A novel strategy for determining a transistor's bias and impedance which simultaneously optimizes these three power metrics was developed. At an initial bias condition, the load and source impedances are tuned to maximize the PAE. Holding these loads constant, the next step determines the optimal bias by measuring two-tone power sweeps. The result is a set of power metric contours across the bias space. The optimal bias condition is determined by analyzing the Pareto front [70]. The optimal bias condition is typically the centroid of the Pareto front polygon.

The strategy was applied to an 83 nm gate length GaN HEMT fabricated and tested at AFRL. Figure 5 shows the load-pull contours measured at 18 dBm input power. A maximum 39.9% PAE was measured at

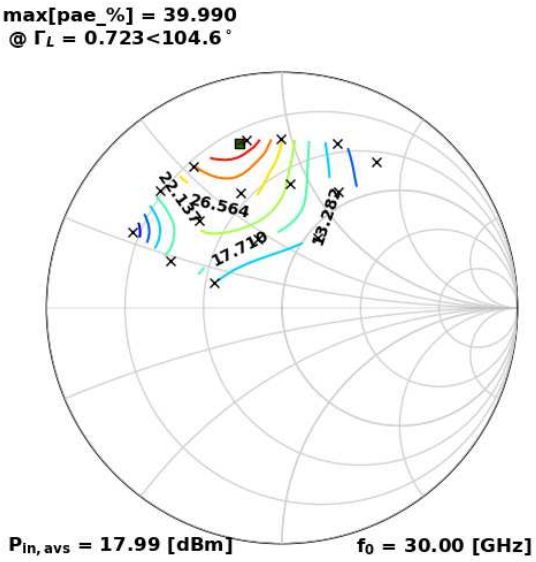

Figure 5: Measured two-tone PAE load-pull contours at 18 dBm available input power and 30 GHz fundamental frequency. The source impedance was $\Gamma_S = 0.25\angle 140°$. The 39.9% peak PAE was measured at $\Gamma_L = 0.72\angle 104°$. These loading conditions were used throughout the bias optimization.

the optimal load conditions $\Gamma_S = 0.25\angle 140°$ and $\Gamma_L = 0.72\angle 104°$. All subsequent power measurements were conducted at these tuning points.

Input power sweeps were then performed for different quiescent bias conditions. Figure 6 shows the maximum output power, maximum PAE, and minimum 3rd order intermodulation (OIP3) as referenced to

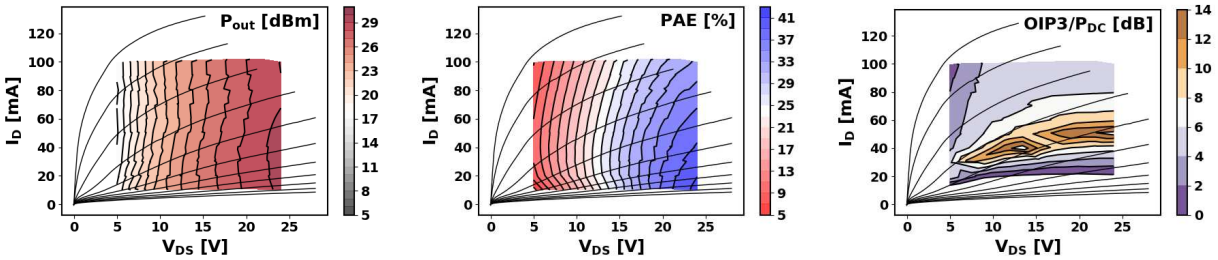

Figure 6: Measured two-tone P_{out} (left), PAE (middle), and OIP3 (right) contours across the I-V plane at 30 GHz fundamental frequency.

the DC power. These measured data produce a Pareto optimal bias condition maximizing all three power metrics of $V_{DS} = 25$ V and $I_D = 45$ mA and indicate a useful strategy for identifying conditions for peak MMIC performance. Further research will investigate implementing this strategy through FKT/DVSI device simulation, circumventing the costly device fabrication and experimental characterization.

4 Conclusion

Satisfying Air Force requirements for high power and high frequency microelectronic and opto-electronic components and systems requires exploring a wide diversity of material systems as well as device and circuit architectures. Surveying such an enormous design space can be prohibitively expensive and time consuming when done solely through an experimental fabrication-testing-redesign process. This lab task endeavors to help meet Air Force technological requirements by developing computational methods and tools capturing the essential physics governing these multi-scale design problems.

The microscopic properties of electronic materials have been treated in various ways depending on crystal complexity. Standard $\boldsymbol{k}\cdot\boldsymbol{p}$ and empirical pseudopotential methods provide accurate electronic band structures for diamond and zincblende lattices like Si and GaAs. Electron-phonon interactions in these materials can also be treated with sufficient accuracy using simple phonon spectra and scattering rates computed from deformation potentials. Other more complex lattices such as wurtzite GaN and monoclinic β-Ga_2O_3 may require ab initio methods such as density functional theory. Recent work with the more computationally efficient density functional tight binding approach has shown it useful for computationally intensive processes such as point defect formation.

Work on this LRIR has resulted in new ways to incorporate the microscopic material properties into device level simulations. Treating mobile charges as ideal Fermi gases provides a numerically efficient and robust hot electron model that can accommodate electronic band structure through integrals of energy dispersion and scattering rates over surfaces of constant electron energy. Further generalization included the field enhanced quantum mechanical tunneling ionization of deep crystal defects. The resulting simulation showed that highly nonlinear tunneling probabilities combined with hot electron effects offer a new theory of an operational instability called the kink effect that has plagued GaN HEMT power amplifiers for over twenty years.

Determining how a simulated device will perform within a highly integrated circuit represents still another level of the multi-scale design problem, a macro-level requiring empirical and computationally efficient compact models. This lab task investigates the many varieties of these behavioral models and is looking toward charge control models to import the results of simulations based on first principal physics into the integrated circuit domain. Recent work has established a device characterization protocol to determine optimum bias conditions for GaN HEMT power applications. Continued research will try implementing this protocol within the lab task's FKT device simulator to demonstrate a full atoms-to-circuits computational design problem.

References

[1] N. Zhang, V. Mehrotra, S. Chandrasekaran, B. Moran, L. Shen, U. Mishra, E. Etzkorn, and D. Clarke, "Large Area GaN HEMT Power Devices for Power Electronic Applications: Switching and Temperature Characteristics," *Power Electronics Specialist Conf.*, vol. 1, pp. 233–237, 2003

[2] Y.F. Wu, B.P. Keller, S. Keller, D. Kapolnek, P. Kozodoy, S.P. Denbaars, and U. Mishra, "High Power AlGaN/GaN HEMTs for Microwave Applications," *Solid-State Electron.*, vol. 41, pp. 1569–1574, 1997.

[3] M.D. Hodge, R. Ventury, J. Shealy, and R. Adams, "A Robust AlGaN/GaN HEMT Technology for RF Switching Applications," *Proc. Compound Semicond. Integr. Circ. Symp.*, pp. 1–4, 2011.

[4] S.M. Goodnick and M. Sarantiti, "Modeling and Simulation of Terahertz Devices," *IEEE Microw. Mag.*, pp. 36–44, Nov./Dec. 2012.

[5] W.P. Pallmann, C.A. Zaugg, M. Mangold, I. Dahhan, M. Golling, B.W. Tilma, B. Witzigmann, and U. Keller, "Ultrafast Electrically Pumped VECSELs," *IEEE Photonics Journal*, vol. 5, no. 4, pp. 1–8, Aug. 2013.

[6] R.G. Bedford, T. Dang, and D. Tomich, "Recent VECSEL Developments for Sensors Applications," *Proc. SPIE*, vol. 8242, San Francisco, CA 2012, pp. 1–8.

[7] C. Jirauschek and T. Kubis, "Modeling Techniques for Quantum Cascade Lasers," *Appl. Phys. Rev.*, vol. 1, pp. 011307–011361, 2014.

[8] R.F. Curl, F. Capasso, C. Gmachl, A.A. Kosterev, B. McManus, R. Lewicki, M. Pusharsky, G. Wysocki, F.K. Tittel, "Quantum Cascade Lasers in Chemical Physics," *Chem. Phys. Lett.*, vol. 487, pp.1–18, 2010.

[9] B.S. Williams, "Terahertz Quantum Cascade Lasers," *Nature Photonics*, vol. 1, Sept. 2007.

[10] H.-B. Liu, H. Zhong, N. Karpowicz, Y. Chen, and X.-C. Zhang, "Terahertz Spectroscopy and Imaging for Defense and Security Applications," *Proc. IEEE*, vol. 95, no. 8, Aug. 2007.

[11] J. Darmo, V. Tamosiunas, G. Fasching, J. Kröll, K. Unterrainer, M. Beck, M. Giovannini, J. Faist, C. Kremser, and P. Debbage, "Imaging with a Terahertz Quantum Cascade Laser," *Opt. Exp.*, vol. 12, pp. 1879–1884, 2004.

[12] H.-W. Hübers, S.G. Pavlov, H. Richter, A.D. Semenov, L. Mahler, A. Tredicucci, H.E. Beere, and D.A. Ritchie, "High-resolution Gas Phase Spectroscopy with a Distributed Feedback Terahertz Quantum Cascade Laser," *Appl. Phys. Lett.*, vol. 89, 061115 (3 pp.), 2006.

[13] M. Lee and M.C. Wanke, "Applied Physics: Searching for a Solid-state Terahertz Technology," *Science*, vol. 316, pp. 64–65, 2007.

[14] E. Pickwell and V.P. Wallace, "Biomedical Applications of Terahertz Technology," *J. Phys. D: Appl. Phys.*, vol. 39, pp. R301–R310, 2006.

[15] M. Cohen and T. Bergstresser, "Band Structures and Pseudopotential Form Factors for Fourteen Semiconductors of the Diamond and Zincblende Structures," *Phys. Rev.*, vol. 141, no. 2, pp. 789–796, 1966.

[16] P. Harrison, **Quantum Wells, Wires, and Dots**, John Wiley & Sons, New York, 2000.

[17] K. Hess, **Advanced Theory of Semiconductor Devices**, IEEE Press, Piscataway, NJ, 2000.

[18] H. Shichijo and K. Hess, "Band-structure-dependent Transport and Impact Ionizatino in GaAs," *Phys. Rev. B*, vol. 23, no. 8, pp. 4197–4207, 1981.

[19] M. Mohamed, I. Unger, C. Janowitz, R. Manzke, Z. Galazka, R. Uecker, and R. Fornari, "The Surface Band Structure of β-Ga_2O_3," *J. of Phys.: Conf. Series*, vol. 286, pp. 012027, 2011.

[20] H. Peelaers and C.G. Van de Walle, "Brillouin Zone and Band Structure of β-Ga_2O_3," *Phys. Status Solidi B*, vol. 252, no. 4, pp. 828–832, 2015.

[21] N. Marzari and D. Vanderbilt, "Maximally Localized Generalized Wannier Functions for Composite Energy Bands," *Phys. Rev. B*, vol. 56, no. 20, pp. 12847–12865, Nov. 1997.

[22] D. Schreurs, M. O'Droma, A.A. Goacher, M. Gadringer, **RF Power Amplifier Behavioral Modeling**, Cambridge University Press, Cambridge, 2009.

[23] L. Dunleavy, C. Baylis, W. Curtice, and R. Connick, "Modeling GaN: Powerful but Challenging," *IEEE Microwave Magazine*, vol. 11, no. 6, pp. 82–96, Oct. 2010.

[24] T. Gasseling, "Compact Transistor Models: The Roadmap to First-Pass Amplifier Design Success," *Microwave Journal*, vol. 13, no. 2, pp. 74–81, March 2012.

[25] U. Radhakrishna, T. Imada, T. Palacios, and D. Antoniadis, "MIT Virtual Source GaNFET-high Voltage (MVSG-HV) Model: A Physics Based Compact Model for HV-GaN HEMTs," *Phys. Status Solidi C*, vol. 11, no. 3-44, pp. 848–852, 2014.

[26] H.-F. Wu, Q.-F. Cheng, S.-X. Yan, Q.-J. Zhang, and J.-G. Ma, "Transistor Model Building for a Microwave Power Heterojunction Bipolar Transistor," *IEEE Microwave Magazine*, vol. 16, no. 2, pp. 85–92, March 2015.

[27] Manel Charfeddine, Hafedh Belmabrouk, Mohamed Ali Zaidi, and Hassen Maaref, "2-D Theoretical Model for Current-voltage Characteristics in AlGaN/GaN HEMTs," *J. of Mod. Phys.*, vol. 3, pp. 881–886, 2012.

[28] Wondwosen Eshetu Muhea, Fetene Mulugeta Yigletu, Roger Cabrë-Rodon, and Benjamin Iñiguez, "Analytical Model for Schottky Barrier Height and Threshold Voltage of AlGaN/GaN HEMTs With Piezoelectric Effect," IEEE Trans. Electron Dev., vol. 65, no. 3, March 2018.

[29] Y. Li, M. Vilathgamuwa, T. Farrell, S.S. Choi, N.T. Tran, and J. Teague, "A Physics-based Distributed-parameter Equivalent Circuit Model for Lithium-ion Batteries," *Electrochimica Acta*, vol. 299, pp. 451–469, Jan. 2019.

[30] , C. Wang, H. Liao, Y. Xiong, C. Li, R. Huang, and Y. Wang, "A Physics-based Equivalent-circuit Model for On-chip Symmetric Transformers with Accurate Substrate Modeling," *IEEE Trans. Microwave Theory Tech.*, vol. 57, no. 4, pp. 980–990, April 2009.

[31] J. Verspecht and D.E. Root, "Polyharmonic Distortion Modeling," *IEEE Microwave Magazine*, vol. 7, no. 3, pp. 44–57, June 2006.

[32] D.E. Root, "Future Device Modeling Trends," *IEEE Microwave Magazine*, pp. 45–59, Nov./Dec. 2012;

[33] J. Verspecht, D. Gunyan, J. Horn, J. Xu, A. Cognata, and D.E. Root, "Multi-tone, Multi-port, and Dynamic Memory Enhancements to PHD Nonlinear Behavioral Models from Large-signal Measurements and Simulations," pp. 969–972, 2007.

[34] D.E. Root, J. Verspecht, D. Sharrit, J. Wood, and A. Cognata, "Broad-band Poly-harmonic Distortion (PHD) Behavioral Models from Fast Automated Simulations and Large-signal Vectorial Network Measurements," *IEEE Trans. Microwave Theory and Tech.*, vol. 53, no. 11 pp. 3656–3664, 2005.

[35] C.-S. Chiu, K.-M. Chen, G.-W. Huang, C.-H. Hsiao, K.-H. Liao, W.- L. Chen, S.-C. Wang, M.-Y. Chen, Y.-C. Yang, K.-L. Wang, and L.-K. Wu, "Characterization of Annular-structure RF LDMOS Transistors Using Polyharmonic Distortion Model," in *IEEE MTT-S Int. Microwave Symp. Dig.*, Jun. 2009, pp. 977980.

[36] G. Simpson, J. Horn, D. Gunyan, and D. E. Root, "Load-pull + NVNA = Enhanced X-parameters for PA designs with High Mismatch and Technology-independent Large-signal Device Models," in *Proc. IEEE ARFTG Conf.*, Portland, OR, Dec. 2008, pp. 88–91.

[37] J. Horn, D.E. Root, and G. Simpson, "GaN Device Modeling with X-parameters," in *Proc. IEEE Compound Semiconductor Integrated Circuits Symp.*, 2010, pp. 1–4.

[38] J.G. Leckey, "A Scalable X-parameter Model for GaAs and GaN FETs," in *Proc. European Microwave Integrated Circuits Conf.*, 2011, pp. 1316.

[39] D.E. Root, M. Marcu, J. Horn, J. Xu, R.M. Biernacki, and M. Iwamoto, "Scaling of X-parameters for Device Modeling," in *Proc. IEEE Int. Microwave Symp.*, Jun. 2012, pp. 1–3.

[40] A. Soury and E. Ngoya, "Handling Long-term Memory Effects in X-parameter Model," *IEEE MTT-S International Microwave Symposium Digest*, Montreal, QC, June 2012.

[41] Y. Wang, T.S. Nielsen, O.K. Jensen, and T. Larsen, "GaN HEMT Device Modeling Using X-parameters with Emphasis on Complexity Reduction of Harmonic Load-pull Measurement," *IEEE Intern. Symp. Signals, Circuits, and Systems*, Iasi, Romania, pp. 1–6, July 2015.

[42] Y. Wang, T.S. Nielsen, O.K. Jensen, and T. Larsen, "X-parameter Based GaN Device Modeling and Its Application to a High-efficiency PA Design," *IEEE Intern. Conf. Numerical Electromagnetic Modeling and Optimization for RF*, Pavia, Italy, pp. 1–4, May 2014.

[43] S. Goasguen and S.M. El-Ghazaly, "A Practical Large-Signal Global Modeling Simulation of a Microwave Amplifier Using Artificial Neural Network," *IEEE Microwave and Guided Wave Lett.*, vol. 10, p. 273, 2000.

[44] C.J. Zhang and K.C. Gupta, **Neural Networks for RF and Microwave Design**, Norwood, MA: Artech House, 2000.

[45] A.H. Zaabab, Q.J. Zhang, and M. Nakhla, "A Neural Network Modeling Approach to Circuit Optimization and Statistical Design," *IEEE Trans. Microwave Theory Tech.*, vol. 43, p. 1349, 1995.

[46] S. Geller, "Crystal Structure of β-Ga_2O_3," *J. Chem. Phys.*, vol. 33, pp. 676–684, 1960.

[47] M. Fleischer and H. Meixner, "Gallium Oxide Thin Films: A New Material for High-temperature Oxygen Sensors," *Sens. Actuators B*, vol. 4, pp. 437–441, 1991.

[48] M. Higashiwaki, K. Sasaki, A. Kuramoto, T. Masui, and S. Yamakoshi, "Gallium Oxide Metal Semiconductor Field-effect Transistors on Single-crystal β-Ga_2O_3 (001) Substrate," *Appl. Phys. Lett.*, vol. 100, p. 013504, 2012.

[49] M. Higashiwaki, K. Sasaki, T. Kamimura, M.H. Wong, D. Krishnamurthy, A. Kuramoto, T. Masui, and S. Yamakoshi, "Depletion-mode Ga_2O_3 Metal-oxide-semiconductor Field-effect Transistors on β-Ga_2O_3 Substrates and Temperature Dependence of their Device Characteristics," *Appl. Phys. Lett.*, vol. 103, p. 123511, 2013.

[50] T. Zacherle, P.C. Schmidt, and M. Martin, "Ab Initio Calculations on the Defect Structure of β-Ga_2O_3," *Phys. Rev. B*, vol. 87, p. 235206, 2013.

[51] A.S. Christensen, T. Kuba, Q. Cui, and M. Elstner, "Semiempirical Quantum Mechanical Methods for Noncovalent Interactions for Chemical and Biochemical Applications," *Chem. Rev.*, vol. 116, pp. 5301–5337, 2016.

[52] J.C. Slater and G.F. Koster, "Simplified LCAO method for the periodic potential problem," *Phys. Rev.*, vol. 94, pp. 1498–1524, 1954.

[53] J.B. Varley, J.R. Weber, A. Janotti, and C.G. Van de Walle, "Oxygen vacancies and donor impurities in β-Ga_2O_3," *Appl. Phys. Lett.*, vol. 97, p. 142106, 2010.

[54] D.J. Meyer, D.A. Deen, D.F. Storm, M.G. Ancona, D.S. Katzer, R. Bass, J.A. Roussos, B.P. Downey, S.C. Binari, T. Gougousi, T. Paskova, E.A. Preble, and K.R. Evans, "High electron velocity submicrometer AlN/GaN MOS-HEMTs on freestanding GaN substrates," *IEEE Electron Device Lett.*, vol. 34, no. 2, pp. 199–201, Feb. 2013.

[55] O. Ambacher, J. Smart, J.R. Shealy, N.G. Weimann, K. Chu, M. Murphy, W.J. Schaff, L.F. Eastman, R. Dimitrov, L. Wittmer, M. Stutzmann, W. Rieger, and J. Hilsenbeck, "Two-dimensional electron gases induced by spontaneous and piezoelectric polarization charges in N- and Ga-face AlGaN/GaN heterostructures," *J. Appl. Phys.*, vol. 85, no. 6, pp. 3222–3233, March 1999.

[56] M. Kuzuhara and M. Tokuda, "Low-loss and high-voltage III-nitride transistors for power switching applications," *IEEE Trans. Electron Devices*, vol. 62, no. 2, pp. 405–413, Feb. 2015.

[57] T.J. Flack, B.N. Pushpakaran, and S.B. Bayne, "GaN technology for power electronic applications: A review," *J. Electron. Mater.*, vol. 45, no. 6, pp. 2673–2682, Jun. 2016.

[58] U.K. Mishra, L. Shen, T.E. Kazior, and Y.-F. Wu, "GaN-based RF power devices and amplifiers," *Proc. IEEE*, vol. 96, no. 2, pp. 287–305, Feb. 2008.

[59] U.K. Mishra, P. Parikh, and Y.-F. Wu, "AlGaN/GaN HEMTs: An overview of device operation and applications," *Proc. IEEE*, vol. 90, no. 6, pp. 1022–1031, June 2002.

[60] R.S. Pengelly, S.M. Wood, J.W. Milligan, S.T. Sheppard, and W.L. Pribble, "A review of GaN on SiC high electron-mobility power transistors and MMICs," *IEEE Trans. Microwave Theory and Tech.*, vol. 60, no. 6, pp. 1764–1783, June 2012.

[61] M. Wang and K.J. Chen, "Kink Effect in AlGaN/GaN HEMTs Induced by Drain and Gate Pumping," *IEEE Electron Device Lett.*, vol. 32, no. 4, pp. 482–484, April 2011.

[62] J.K. Kaushik, V.R. Balakrishnan, B.S. Panwar, and R. Muralidharan, "On the origin of kink effect in current-voltage characteristics of AlGaN/GaN high electron mobility transistors," *IEEE Trans. Electron Devices*, vol. 60, no. 10, pp. 3351–3357, Oct. 2013.

[63] G. Meneghesso, F. Zanon, M.J. Uren, and E. Zanoni, "Anomalous kink effect in GaN high electron mobility transistors," *IEEE Electron Dev. Lett.*, vol. 30, no. 2, pp. 100–102, Feb. 2009.

[64] M. Xiao-Hua, L. Min, P. Lei, J. Yuan-Qi, Y. Jing-Zhi, C. Wei-Wei, and L. Xin-Yu, "Kink effect in current-voltage characteristics of a GaN-based high electron mobility transistor with an AlGaN back barrier," *Chin. Phys. B*, vol. 23, no. 2, pp. 027302-1–027302-4, 2014.

[65] M. Singh, M.J. Uren, T. Martin, S. Karboyan, H. Chandrasekar, and M. Kuball, "'Kink' in AlGaN/GaN-HEMTs: Floating buffer model," *IEEE Trans. Electron Devices*, vol. 65, no. 9, Sep. 2018.

[66] H. Hirshy, M. Singh, M.A. Casbon, R.M. Perks, M.J. Uren, T. Martin, M. Kuball, and P.J. Tasker, "Evaluation of pulsed IV analysis as validation tool of nonlinear RF models of GaN-based HFETs," *IEEE Trans. Electron Devices*, vol. 65, no. 12, pp. 5307–5313, Dec. 2018.

[67] P. Altuntas, N. Defrance, M. Lesecq, A. Agboton, R. Ouhachi, E. Okada, C. Gaquiere, J.-C. De Jaeger, E. Frayssinet, and Y. Cordier, "On the correlation between kink effect and effective mobility in InAlN/GaN HEMTs," *Proc. 9th European Microw. Integrated Circuits Conf.*, Rome, Italy, Oct. 2014, pp. 88–92.

[68] C. Sharma, R. Laishram, Amit, D.S. Rawal, S. Vinayak, and R. Singh, "Investigation on de-trapping mechanisms related to non-monotonic kink pattern in GaN HEMT devices," *AIP Advances*, vol. 7, pp. 085209-1–085209-5, Aug. 2017.

[69] M. Grupen, "Reproducing GaN HEMT Kink Effect by Simulating Field Enhanced Barrier Defect Ionization," *IEEE Trans. Electron Dev.*, vol. 66, no. 9, pp. 3777–3783, Sept. 2019.

[70] J. Martin, C. Baylis, L. Cohen, J. de Graaf, and R.J. Marks II, "A Peak-search Algorithm for Load-pull Optimization of Power-added Efficiency and Adjacent-channel Power Ratio," *IEEE Trans. Microwave Theory and Tech.*, vol. 62, no. 8, pp. 1772–1783, Aug. 2014.

Appendix A: In-House Activities

Personnel:

Name	Emp. Type	Field	Role	Involvement
Dr. M. Grupen	Civ.	Electrical Engineering	Theory & Sim.	60%
Dr. N. Miller	Civ.	Electrical Engineering	Theory & Sim	40%
Dr. S. Badescu	Civ.	Physics	Theory & Sim	35%
Dr. N. Usechak	Civ.	Optical Engineering	Theory & Sim	5%

Publications:

1. **M. Grupen**, "Reproducing GaN HEMT Kink Effect by Simulating Field Enhanced Barrier Defect Ionization," *IEEE Transactions on Electron Devices*, vol. 66, no. 9, pp. 3777–3783, Sept. 2019. https://doi.org/10.1109/TED.2019.2928536

2. D. Hashemi, G. Siegel, M. Snure, **S.C. Badescu**, "Vicinal Metal Surfaces as Potential Catalysts for Phosphorene Epitaxial Growth," *Applied Physics Letters*, vol. 115, no. 11, pp. 113104-1–113104-5, Sept. 2019. https://doi.org/10.1063/1.5114629

3. M. Snure, T. Prusnick, E. Bianco, **S.C. Badescu**, "A Computational and Experimental Investigation of the Phonon and Optical Properties of Au_2P_3," *Materials*, vol. 12, no. 4, pp. 555–562, Feb. 2019. https://doi.org/10.3390/ma12040555

4. J. Lee, S. Ganguli, A.K. Roy, and **S.C. Badescu**, "Density Functional Tight Binding Study of βGa_2O_3: Electronic Structure, Surface Energy, and Native Point Defects," *Journal of Chemical Physics*, vol. 150, no. 17, pp. 174706-1–174706-8, May 2019. https://doi.org/10.1063/1.5088941

5. **N.C. Miller**, **M. Grupen**, K. Beckwith, D. Smithe, and J.D. Albrecht, "Computational Study of Fermi Kinetics Transport Applied to Large-signal RF Device Simulations," *Journal of Computational Electronics*, vol. 17, no. 4, pp. 1658–1675, Dec. 2018. https://doi.org/10.1007/s10825-018-1242-5

Presentations:

1. **C.S. Badesc**, invited talk "Modeling of phase transitions in aluminum-gallium oxide alloys," Proceedings of SPIE, vol. 10919 Oxide-based Materials and Devices X, San Francisco, CA, March 2019. https://doi.org/10.1117/12.2514838

2. **M. Grupen**, **N.C. Miller**, and J. Albrecht, "Investigating the 'Kink Effect' in GaN HEMT Technology Using Fermi Kinetics Transport," *20th International Workshop on Computational Nanotechnology*, Evanson, Illinois, May 2019.

3. **N.C. Miller**, N. Moser, G.D. Via, R. Fitch, J. Gillespie, A. Green, D. Walker, Jr., A. Crespo, M. Schuette, and K. Chabak, "Optimizing the Bias and Impedance Trade Space for High Power and High Linearity GaN HEMTs," submitted to GOMACTech 2020, San Diego, CA, March 2020.

Professional Activities:

IEEE Dayton Section Harrel V. Nobel Award for physics-based modeling (Miller)

Team Lead for DARPA DREaM verification and validation measurement group (Miller)

Scientific Advisory Board Best Presentation Award, "Physics-based Device Modeling" (Miller)

Manager of in-house GaN140 PDK (Miller)

Managing in-house ASM-HEMT model development with contractor Keysight Technologies (Miller)

Program Officer for "High Speed Electronic Device Simulator" STTR Phase 2 awarded to TechX/Michigan State University (Miller)

NRC Research Advisor (Grupen, Badescu, Usechak)

IEEE Electron Device Letters reviewer (Miller)

Managed KPP measurements and evaluations of GaN transfer Mantech effort (Miller)

DoD HPCMP project manager (Miller)

Managing Keysight ADS PDK for the in-house GaN process (Miller)

Technical Advisor for SOCHE student Bendic Pacia (Miller, Grupen)

Reviewer for AFOSR computer simulation proposals (Grupen)

Advisor for on-site Post-doctoral Fellow Dr. Daniel Hashemi (Badescu)

Advisor for on-site Post-doctoral Fellow Dr. Marco Santia (Badescu)

IEEE AVFOP GOMAC Session Chair, Albuquerque, NM (Usechak)

Optics Letters reviewer (Usechak)

Optics Express reviewer (Usechak)

Journal of Selected Topics in Quantum Electronics reviewer (Usechak)

Government Program Manager and CTO for $112.5M AIM Photonics Program (Usechak)

Reviewer, SME, and Contract Officer Representative for DARPA/STO (Usechak)

Reviewer, SME, and Contract Officer Representative for DARPA/MTO (Usechak)

Author and Program Manager for $2.25M SBIR Phase II topic "Scalable Coherent Photonic Array on a Silicon Platform" (Usechak)

Author and Program Manager for $10.55M SBIR Phase III topic "Coherent Homodyne Integrated RF-photonic Systems (CHIPS)" (Usechak)

Author and Program Manager for $10.55M SBIR Phase III topic "40 GHz Instantaneious Wideband Spectrum Monitoring System" (Usechak)

Author and Program Manager for AFRL's $6M RIPTIDE Program spread over four different contracts (Usechak)